JSST

Vol.15 / Special Issue / 2022 / (No. 51)
Print ISSN: 2008-4560 / Online ISSN: 2423-4516
https://doi.org/10.30699/jsst.2022.1156

Pages: 1-13 / Research Paper / Received: 12 December 2018 / Revised: 08 July 2019 / Accepted: 23 October 2019

Journal Homepage: https://jsst.ias.ir

Effects of Geometrical Parameters of Gas Flow Channels on Polymer Electrolyte Membrane Fuel Cell Performance

Hamed Moeini[1]*, Ebrahim Afshari[2] and Karim Mazaheri[3]

1. Department of Aerospace Engineering, Sharif University of Technology, Tehran, Iran
2. Department of Mechanical Engineering, Faculty of Engineering, University of Isfahan, Isfahan, Iran
3. Faculty of Aerospace Department, Sharif University of Technology, Tehran, Iran

*Corresponding Author's E-mail: hamedm_313@yahoo.com

Abstract

In the present study, the effects of geometrical properties of gas flow channels on both current density and temperature distributions inside a polymer electrolyte membrane (PEM) fuel cell are investigated. The main purpose here is to clarify the effects of the variation of width, depth, and the ribs of flow channels on the fuel cell performance. To do this, the fuel cell is numerically simulated in two dimensions. The governing equations consist of the conservation of the electrical potential, Darcy's law as alternative to the momentum equation, Maxwell-Stefan equation for mass transport, energy conservation, and electro-thermal equations along with the Butler–Volmer equation. Numerical results indicate that the width of channels and their ribs have more sensible effects than the depth of flow channels on the current density and temperature distributions and fuel cell performance. While the maximum temperature of the cell is increased by increasing the width of the flow channels, the current density distribution and fuel cell performance can be improved. By decreasing the width of their ribs or depth of channels, the performance of the fuel cell is improved and its maximum temperature is decreased.

Keywords: Polymer electrolyte membrane fuel cell, Membrane, Electrodes, Current density, Temperature distribution

Nomenclature

k_p	permeability
η	fluid viscosity
T	temperature in Kelvin
ω	mass fraction
x	mole fraction
D_{ij}	diffusion coefficient
D_i^T	transpose of the diffusivity coefficient matrix
R_i	velocity of reacting matters
M	molecular weight
R	universal gas constant
P	Pressure
J^e	external current density
Q_j	electrical current source
ρ_0	resistance at a reference temperature
T_0	reference temperature
$k^{m,eff}$	effective conductivity of membrane
$k^{s,eff}$	effective conductivity of electrodes
ϕ_s	Electrical potential in the electrode
ϕ_m	Electrical potential in the membrane

Introduction

A typical fuel cell is an electrochemical equipment converting the chemical energy into the electrical energy.

1. M.Sc.
2. Associate Professor
3. Professor

How to cite this article:
H. Moeini, E. Afshari, and K. Mazaheri, " Effects of Geometrical Parameters of Gas Flow Channels on Polymer Electrolyte Membrane Fuel Cell Performance," *Journal of Space Science and Technology*, Vol. 15, Special Issue, pp. 1-13, 2022, https://doi.org/10.30699/jsst.2022.1156.

The chemical energy is released due to the chemical reaction of a fuel and a substance as an oxidizer. While the reactive gases are provided, fuel cells can continuously convert the chemical energy into the electrical one, unlike batteries which release the stored chemical energy. Among different types of fuel cells, the polymer electrolyte membrane (PEM) fuel cell is the most commonly used one, as they have high efficiency and the current density values along with variety and quick start-up time [1, 2].

Dimensions and the pattern of the flow channels can have noticeable effects on the transportation and consumption of the reactive gases, water management, and the fuel cell performance [3]. If the amount of the output water and gas gets out of control, the oxygen transfer rate toward the catalyst layer is dramatically decreased. This may lead to an overheated fuel cell and a dried membrane in some cases. This unwanted situation increases the internal resistance of the cell which decreases the fuel cell performance. Thus, an optimal design of the fluid flow channels is vital in order to guarantee the nearly uniform distribution of the reactive gases and temperature in the fuel cell. In addition, the performance and lifetime of the PEM fuel cells highly depend on the structure of the flow field. Therefore, the design of flow channels is a challenge in the designing procedure of the PEM fuel cells [4].

A typical and desirable flow field for an ideal PEM fuel cell has the following basic properties:

1. Sufficient amount and uniform distribution of the reactive gases are available in the catalyst layer.
2. The products of the chemical reaction are completely exhausted from the flow channels to the outside of the fuel cell.
3. A proper electron exchange between the gas diffusion and catalyst layers is performed.
4. Minimum pressure drop along the flow channels is observed.
5. There exists a uniform temperature distribution within the PEM fuel cell.

During the past years, several researchers have attempted to design or to select proper fluid flow channels for the PEM fuel cells. The various structures for the flow channels have been proposed, developed, and used, including the parallel, single, and multiple serpentine, pin-type flow channels along with channels with specific profiles with their own properties, advantages, and disadvantages [5-7]. The concentration and distribution of reactants, the reaction rate of the chemical reactions at catalyst layer, along with temperature distribution inside the electrodes highly depend on the flow channel structure. Thus, designing the fluid flow channels of the fuel cells is a vital key to reach a fuel cell with a high performance and the five mentioned properties.

The performance of a PEM fuel cell is influenced by two main factors including operating conditions (operating temperature, operating pressure, the reactants flow rate, and reactants humidity) and the geometrical parameters (shape of the flow field, channel width, rib width, and etc). Effects of these factors on the performance of the fuel cells have been studied by many researchers.

Um et al. modeled a two dimensional fuel cell based on the finite volume approach to investigate the current density values at the catalyst layer and the rate of consumptions of water and the reactants [8]. Owejan et al. studied the accumulation of the produced water at the cathode catalyst layer and flooding effects on the PEM fuel cells. They attempted to resolve these problems using different structures for the flow channels [9].Wan et al. studied the amount of water produced in the catalyst layer, and showed that the water management in the PEM fuel cell plays a very important role in the fuel cell performance. Also, to ensure a high ionic conductivity in the fuel cell electrolyte, it is necessary that the membrane water capacity, especially in high current density, is controlled [10]. Rowshanzamir et al. investigated a parametric study on the current density on the cathode side of the PEM fuel cell, in terms of the oxygen and hydrogen concentrations [11]. Kwac et al. investigated the distributions of reactants and products by numerical simulation of a two dimensional PEM fuel cell model, using the finite element method. In addition, they compared the numerical results with experimental data and discussed about the polarization curve of the PEM fuel cell [12]. Ameriet al. using the COMSOL software and using the Stefan-Maxwell transfer equations, continuity equations and Navier-Stokes equations, modeled the PEM fuel cell in a two-dimensional model [13].

Zhang et al. used single serpentine flow fields with four different land widths in PEM fuel cells and studied the effects of the land width and inlet flow rate on the cell performance. The results showed that the cell performance always increases with the decrease in the land width and the increase in the inlet flow rates [14]. Ahmadi et al. focused on the improvement of the PEM fuel cell performance by changing the geometrical parameters of the cell. In this work, the cross section of the gas channel changed from square to inverse trapezoid and showed that at an equable voltage, this new model of the channels enhances the current density of the fuel cell [15]. Muthuk umar et al numerically studied the effects of different landing to channel width of flow channel on the PEM fuel cell performance. They show that the smaller width of landing and channels are required for high current density outputs of the PEM fuel cell [16]. Liu et al. developed a mathematical model for PEM fuel cell to optimize the dimensions of reactant flow channels and walls/ribs in the cell. The results showed that relatively small widths of reactant flow channels and ribs are preferred for obtaining high current and power densities [17]. Lakshminarayanan and Karthikeyan investigated the effects of operating conditions, design parameters and various rib width to channel width 1:1, 1:2, 2:1, and 2:2 on performance of serpentine and

interdigitated gas flow channel of 25cm^2 area of the PEM fuel cell [18]. Hadjaj and Kaabar present a three-dimensional model for PEM fuel cell to investigate the effects of different shapes of channels on the performance and the transport phenomena in the cell. The simulation results show that at low voltage when channels geometry is triangular, the performance of the cell is better than the rectangular and elliptical channels [19].

In the present study, a geometric study on the fluid flow channels of a typical PEM fuel cell is performed by considering the thermal effects and the temperature distribution in the fuel cell. In addition, the effects of the width and the depth of the flow channels along with distances between the channels on both fuel cell performance and temperature distribution inside the fuel cell are investigated by introducing a number of models for the fuel cell as follows.

Modeling of the PEM Fuel Cell

In a typical PEM fuel cell, the humidified hydrogen and air enter the fuel cells through a number of fluid flow channels at two different regions called the anode and the cathode sides of the fuel cell, respectively. Then, a set of electro-chemical reactions is performed to produce electrical energy, as the main output of the fuel cells, along with water and heat as the by-products. While the anode reaction is relatively endothermic, the cathode reaction is highly exothermic. As a result, heat is generated inside the fuel cell.

Fig. 1 shows a typical cell of the PEM fuel cell with its components. A cell is made of different layers with their own properties and a number of flow channels. At the center of the cell, there is a very thin membrane which should permit merely protons (not electrons) to transfer between the anode and the cathode sides of the cell. According to this property, electrons are forced to move along the external circuit and produce electrical work. On each side of the membrane, there is a catalyst layer. The anode catalyst layer allows hydrogen to be decomposed into two protons (hydrogen ions) and two electrons. The cathode catalyst layer is the region where oxygen reacts with released protons from the anode side to produce water. Outside the catalyst layers, the gas diffusion layers are located. The gas diffusion layer facilitates transport of reactive gases into the catalyst layer and also helps remove the produced water from the cell.

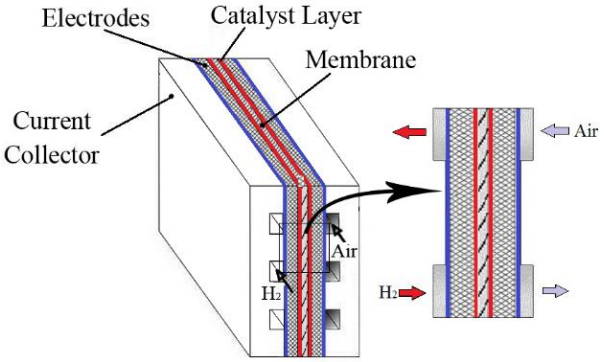

Fig. 1. A typical polymer membrane fuel cell with its components.

The main purpose of the present study is to focus on the effects of geometrical properties of the PEM fuel cell on its performance. To do this, the total number of seven geometries of the fluid flow channels (Geometries A to G) are proposed and compared. These geometries can be classified into four main categories as follows:

1. Geometries considered to study the effects of the width of the flow channels on the fuel cell performance (Geometries A and B).
2. Geometries with various lengths of ribs and constant width of the flow channels (Geometries C and D).
3. Geometries with different depths of flow channels (geometries E and F).
4. A geometry with step-like flow channels (Geometry G).

Geometries A, B, C, E, and F have the same structures, as shown in Fig. 2a. In addition, the structure of the Geometries D and G are shown in Figs. 2b and 2c, respectively. Table 1 summarizes the dimensions associated with each geometry considered for the PEM fuel cell. It should be noted that due to the constraints on channel dimensions that would be very difficult to obtain by machining, the Geometry E (depth channel=0.2 mm) is selected as elementary geometry. Then, the results of all geometries are compared with this geometry.

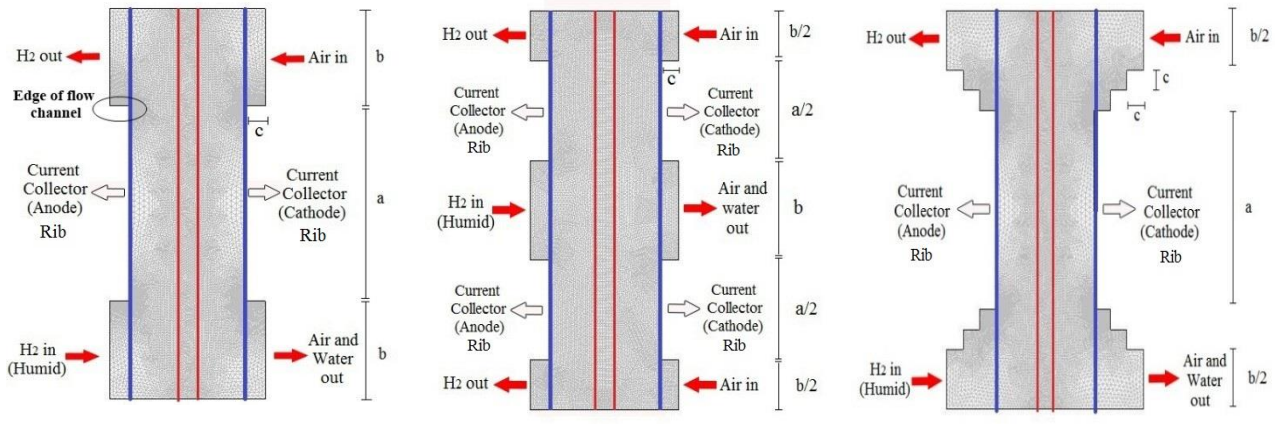

a) **Geometries A, B, C, E, and F** **b)** **Geometry D** **c)** **Geometry G**

Fig. 2. Illustration of different Geometries for the fluid flow channels of the PEM fuel cell.

Table 1. Values of the parameters a, b, and c in different geometries of the fuel cell.

Geometry	a (mm)	b (mm)	c (mm)
A	1.0	0.5	0.1
B	0.5	0.75	0.1
C	1.5	0.25	0.1
D	1.0	0.5	0.1
E	1.0	0.5	0.2
F	1.0	0.5	0.3
G	1.0	0.5	0.1

Governing Equations

To develop a proper mathematical and numerical model for the PEM fuel cell, at first, the following assumptions are considered:

1. The fuel cell operates in steady state conditions.
2. The gas mixtures behave as an ideal gas.
3. As the Reynolds's number is relatively small; the flow regime inside the channels is laminar.
4. According to the velocity and temperature values in the flow channels (0.016 m/s and 353 K), gas flow is assumed to be incompressible.
5. Electrodes, catalyst layers, and membrane are homogeneous and isotropic porous media.

Based on the mentioned assumption, the governing equations associated with a typical PEM fuel cell are simplified. These are the conservation of the mass, momentum, energy, chemical species, and the electrical potential. The continuity equation is given by Equation (1), with respect to the above assumptions:

$$\nabla \cdot (\rho\, u) = 0 \tag{1}$$

The flow is laminar in all regions of the fuel cell and for the momentum study; the Darcy law has been used in porous media [12], this rule is used to calculate the velocity of Equation (2).

$$u = -\frac{k_p}{\eta}\nabla p, \tag{2}$$

Where, k_p is the permeability(m^2) and η is the fluid viscosity (kg/m).

The conservation of species is modeled based on the Stephen Maxwell's equations. Here, the species are hydrogen and water in the anode side and oxygen, nitrogen, and water at the cathode side of the cell. The conservation of species can be mathematically written as [12-14]:

$$\frac{\partial(\rho\omega_i)}{\partial t} + \nabla \cdot \left[-\rho\omega_i \sum_{j=1}^{N} D_{ij}A + \rho\omega_i \boldsymbol{u} + D_i^T \frac{\nabla T}{T}\right] = R_i \tag{3}$$

$$A = \left\{\frac{M}{M_j}\left(\nabla\omega_j + \omega_j \frac{\nabla M}{M}\right) + \left(x_j - \omega_j\right)\frac{\nabla p}{p}\right\}, \tag{4}$$

Here, the parameter T is temperature in (K), ω is mass fraction, and x is mole fraction. Moreover, D_{ij} is diffusion coefficient (m^2/s), D_i^T is the transpose of the diffusivity coefficient matrix, and R_i is the velocity of reacting matters (m/s). In addition, M represents the molecular weight (kg/mol) and ρ is the fluid density (kg/m^3), which can be represented by [12]:

$$\rho = \frac{P.\sum_i x_i M_i}{R.T} \tag{5}$$

Here, P is pressure (kPa), and R is universal constant of gases.

The energy balance equation and electro-thermal equations are used to obtain the temperature distribution inside the fuel cell. The energy equation is given by [20-21]:

$$\rho C_p u \cdot \nabla T = \nabla \cdot (k\nabla T) + q_s \tag{6}$$

where, k is thermal conductivity $(W/m.K)$ and term Q is heat source (W/m^3).

Released heat from the electricity is calculated by the relation below:

$$-\nabla \cdot d(\sigma\nabla V - J^e) = dQ_j\,, \tag{7}$$

$$\sigma = 1/(\rho_0(1 + a(T - T_0))) \tag{8}$$

In the above equation, J^e is external current density (A/m^2), $Q_j$is electrical current source (A/m^3), ρ_0 is resistance at a reference temperature (Ω/m), a is the temperature coefficient $(1/K)$ and $T_0 = 293(K)$ is the reference temperature.

The conservation of electrical potential for anode, membrane, and cathode domains is expressed as [12]:

$$\nabla \cdot (-k^{s,eff}\nabla\phi_s) = 0\,, \tag{9}$$

$$\nabla \cdot (-k^{m,eff}\nabla\phi_m) = 0, \tag{10}$$

$$\nabla \cdot (-k^{s,eff}\nabla\phi_s) = 0\,, \tag{11}$$

Here, the parameters $k^{m,eff}$and $k^{s,eff}$ are the effective conductivity of membrane and electrodes both in (S/m), respectively. $k^{s,eff}$is a function of humidity selected in accordance to the reference model with relative humidity of 100%. In addition, electrical potential in the electrode and membrane phases are ϕ_s (V) andϕ_m, respectively.

Boundary Conditions and Numerical Methods

As the fuel cell has different parts and various parameters, it is generally difficult to study the effects of all parameters of all parts on the fuel cell performance. Here, the layers of rib, flow channels in both anode and cathode sides (blue lines in Figs. 2), and active anode and cathode catalyst layers (red lines in Figs. 2) are considered.

Equations (1) to (11) construct a complete system for describing the physical behavior of the PEM fuel cell. In order to solve these equations, one needs to impose proper boundary conditions; here, it is assumed that all outer boundaries of the fuel cell except for the ribs of the channels are electrically insulated. For each rib of the flow channels, the electrical potential is considered as a boundary condition, in such a way that the electrical potential on the anode and cathode sides are chosen as zero and 0.7 (V), respectively. Based on the Darcy's law, the velocity is expressed in terms of the pressure gradient. Thus, the values of pressure are set as the boundary conditions at the inlet and outlet of the channels. In fact, the velocity values are determined. For the boundaries of the membrane the inflow/outflow boundary conditions are defined. The physical properties of the PEM fuel cell are presented in Table 2. It should be mentioned that, in the present study, it is assumed that water always remains in the vapor phase.

The governing equations along with the mentioned boundary conditions are numerically solved based on the finite element approach, using the COMSOL software [20]. In general, different computational grids are used for different Geometries. For each case, the total number of nodes in the computational grid is chosen in such a way that the results become grid independent. These are 24160, 18560, 26016, 18048, 25760, 25760, and 27264 nodes for the Geometries A to G, respectively. To increase the accuracy of the results, the grid refinement is also performed in the inlet and outlet regions of the gas diffusion layer and flow channels. The governing equations are solved by an iterative numerical algorithm, in the COMSOL software, with a predefined residual, say10^{-6}, as the convergence criteria.

Table 2. The physical, chemical properties of the fuel cell.

Expression	Variable	Value
Conductivity, solid phase	$k^{s,eff}$	*1000 [S/m]*
Conductivity, membrane	$k^{m,eff}$	*9 [S/m]*
Cell voltage	V_{cell}	*0.7 [V]*
Cell Temperature	T	*353 [K]*
Fluid viscosity	H	2.1×10^{-5} *[Pa.s]*
Reference pressure	P_{ref}	1.013×10^{5} *[Pa]*
Inlet pressure, anode	$P_{a,in}$	$1.1 \times P_{ref}$
Inlet pressure, cathode	$P_{c,in}$	$1.1 \times P_{ref}$
Water drag coefficient	*Drag*	*3*
Anode thermal conductivity	k_{anode}	*0.5 [W/m.K]*
Membrane thermal conductivity	$k_{membrane}$	*0.95[W/m.K]*
cathode thermal conductivity	$k_{cathode}$	*0.5[W/m.K]*
Density of anode and cathode	$\rho_{anode}, \rho_{cathod}$	*1890[kg/m3]*
Density of membrane	$\rho_{membrane}$	*1980[kg/m3]*
Heat coefficient at constant pressure	*Cp*	*670[J/kg.K]*

Numerical Results

a) Validation of the Results of Present Study

To validate the numerical results, the polarization curve obtained in the present study in comparison with those reported in Ref [12] are shown in Fig. 3a. Results show that the numerical results of the present study have a good agreement with both numerical and experimental data in such a way that errors are less than 5 and 15%, respectively. In addition, the variation of the current density inside the active catalyst layer is presented in Fig. 3b. It is clear that the numerical results associated with the present study have an acceptable accuracy, especially for moderate and small current density values. Unlike low current densities, the values of potential predicted by numerical results differ from the measured ones for the high current density values (Fig. 3a). The difference in simulation results with experimental results in high-density flow is due to numerical simulation of a fuel cell in a single-phase manner.

b) Comparison of geometries with different width of the flow channels (Geometries A, B)

The distributions of the current density at the PEM fuel cell associated with the Geometries A and B are presented in Figs. 4a and 4b, respectively. As can be seen in both geometries, the current density in regions near the ribs of the channels has the highest values and the current density is decreased by leaving from the ribs of the channels. In addition, the current density is very low at the inlet and outlet of the flow channels.

Moreover, the current density is relatively high in regions bounded between the ribs of the channels and membrane (Figs. 4a and 4b). As an important point, the current density at the edges of current collectors (Fig. 4a) is increased by increasing the width of the flow channels. In fact, for a typical PEM fuel cell with specific dimensions, the size of the intersection of the gas diffusion layer and the flow channels is increased by enlarging the width of the channels. From a physical point of view, as the interspersions of the gas diffusion layer and channels becomes larger, more active gases can penetrate into the gas diffusion layers and finally into the catalyst layers which results in the concentration losses. This can increase the concentration of the reactive gases at the catalyst layers and improve the chemical reaction rate, and consequently, increase the current density value. The

current density inside the active anode layer is shown in Fig. 5 for both Geometries A and B. It is clear that the current density in the Geometry B (with a larger channel width) is generally higher than that of the Geometry A. In fact, as the width of channels becomes larger, the size of intersection of channel/electrode in the anode side is increased. This helps hydrogen to transfer into the anode electrode and increase the consumption rate of hydrogen at the active anode layer. A considerable point is here that the current density of the Geometry A at the anode outlet is higher than that of the Geometry B.

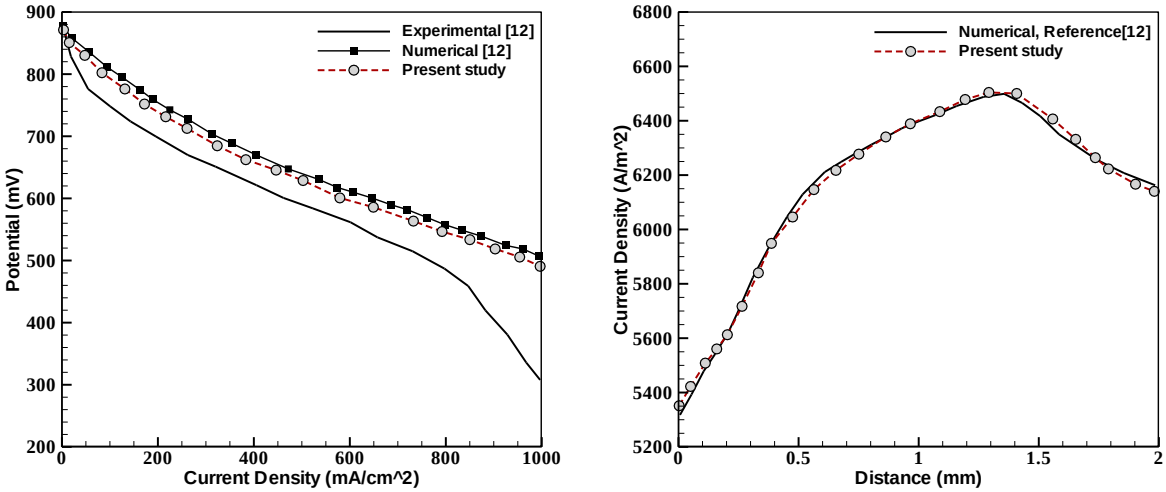

b) Polarization curves **a) Current density inside the active catalyst layer**

Fig. 3. Comparison of the results of the present study with those reported in [12].

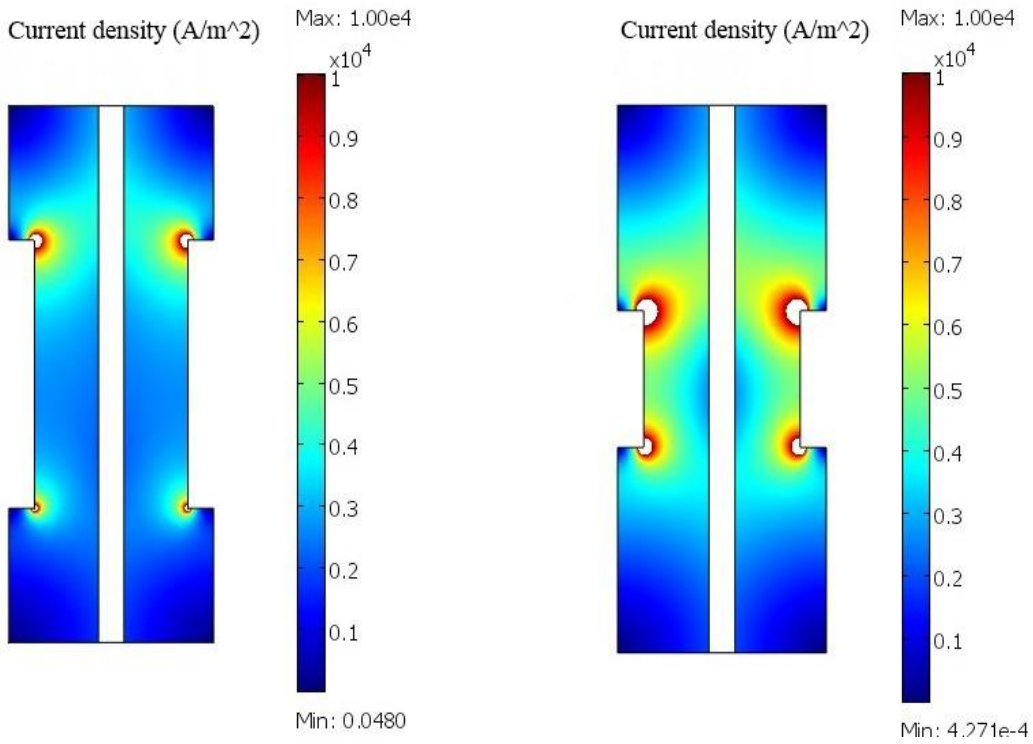

a) Geometry A **b) GeometryB**

Fig. 4. Contours of current density inside the fuel cell.

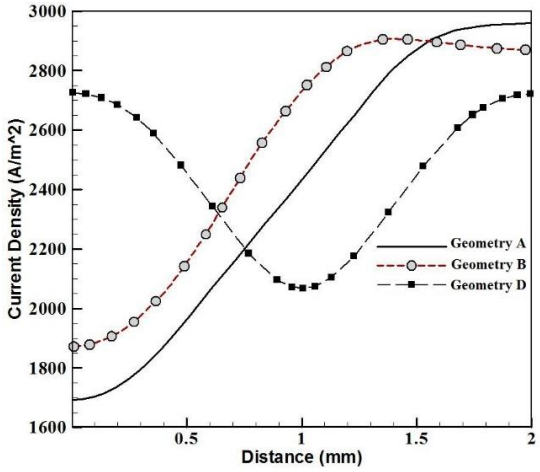

Fig. 5. Current density inside the catalyst layer.

Figs. 6a and 6b show the temperature distribution at the rib and sections of channels on the cathode and anode sides of the fuel cell, respectively. Comparing the geometries, A and B, one can observe that, temperature is decreased by increasing the width of flow channels. Although, the current density is increased by increasing the width of flow channels (Figs. 4a and 4b), the rate of heat generation inside the fuel cells is also increased. Fortunately, the contribution of the convective heat transfer is increased which helps remove the generated heat from the fuel cell. The thickness of the rib in the Geometries A and B is 0.5 and 0.75 (mm), respectively. The temperature in these regions is increased due to increase in the local current density value. Also, because the current density at the edge of the anode output is greater than the current density at the edge of the input side, the temperature in those areas has increased (the widths of channels in Geometries A and B are 1.5 and 1.25 (mm), respectively).
Similar behavior can be seen for the anode side of the fuel cell, as shown in Fig. 6b. The regions near the ribs of the channels have the high temperature value and the temperature of the fuel cell can be decreased by increasing the width of the flow channels. However, the maximum temperature at the anode side is less than that of the cathode side of the fuel cell.

This is because that the generated heat in the chemical reaction on the cathode side is greater than that of the anode side of the fuel cell, due to the cathodic reaction. In addition, H_2 diffusivity on the anode side is greater than O_2 diffusivity on the cathode side. As a result, the concentration losses at the cathode side are greater than that of anode side, and consequently, it has a greater heat generation rate.
The temperature contours at the cross section of fuel cells associated with two Geometries A and B are presented in Figs. 7a and 7b. Comparing these geometries, one can observe that the maximum temperature in the geometry B is relatively less than that of the geometry A. This is an interesting point as one may achieve a minimum variation of temperature inside the fuel cell. The polarization curve of the Geometries A and B are compared in Fig. 8. As a result, the geometry B with higher current density value has a better performance, when compared with geometry A. This means with increasing the width of the flow channels, PEM fuel cell performance can be improved.

C) Comparison of Geometries with Different Width of Ribs of the Flow Channels (Geometries C and D)

In this section, the performance of fuel cells is compared for two geometries C and D. As shown in Fig. 2, the width of the ribs in the geometries C and D are 1.5 and 0.5 (mm), respectively. In addition, the distribution of the current density in these geometries is represented in Fig. 9. In fact, by increasing the width of the ribs, the fewer amounts of hydrogen and oxygen transfer into the gas diffusion and catalyst layers which leads to a decrease in the chemical reaction rate. This means that the current density is decreased by increasing the width of the ribs.

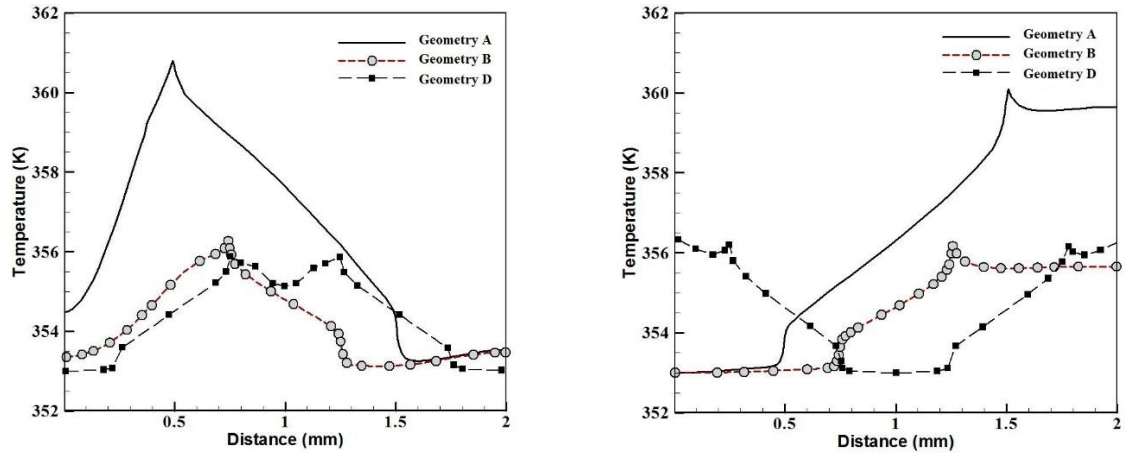

a) Cathode side **b) Anode side**

Fig. 6. Temperature variation between the ribs and channels of the fuel cell

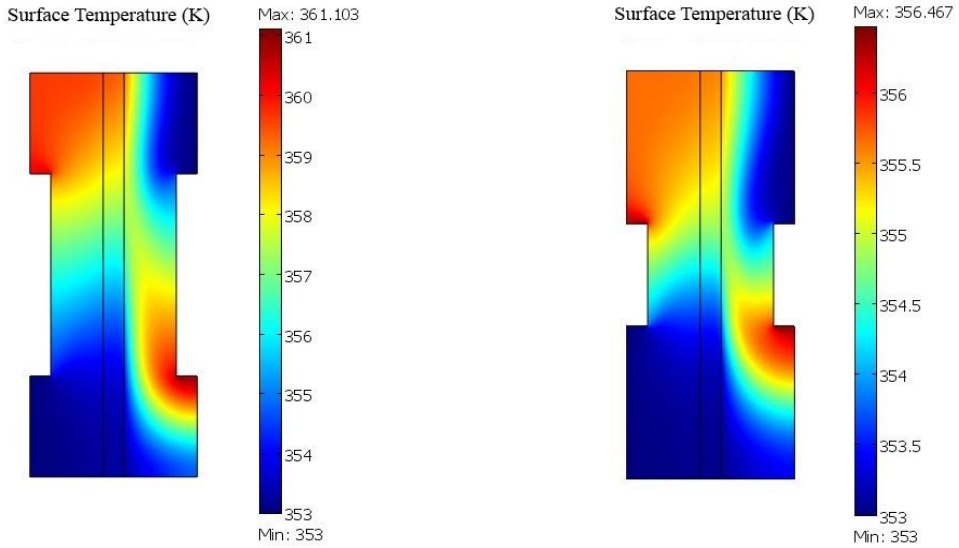

a) GeometryA **b) Geometry B**

Fig. 7. Temperature distributions in the cross section of geometries with different width of channels.

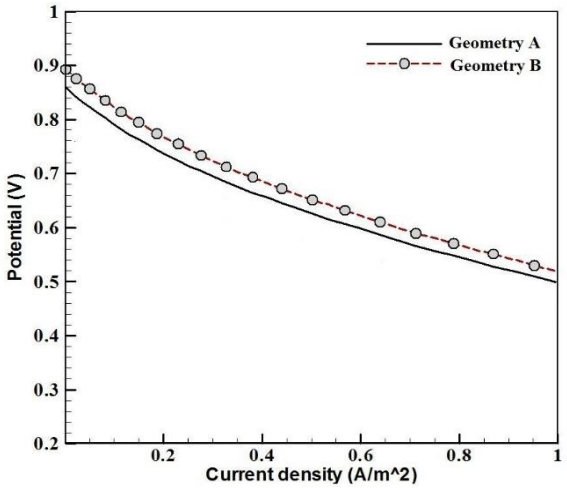

Fig. 8. Comparison of polarization curves for fuel cells associated with geometries A and B.

Note that the current density in regions near the edges of the flow channels (shown in Fig. 2a) for both geometries C and D is relatively high, as enough amount of the reactive gases is available. This leads to an increase in the temperature and also provides a non-uniform temperature distribution inside the fuel cell (Fig. 10). An important point is that the current density distribution in the geometry D is more uniform than that of the geometry C. The uniform current density distribution can result in a more uniform temperature distribution, as illustrated in Figs. 10a and 10b. It can be observed that the maximum temperature is decreased by decreasing the width of ribs in such a way that this value is reduced from 366 (K) to 357 (K) by a three times smaller rib. By decreasing the size of the ribs, the more amount of heat is transferred by the reactive gases through convection outside the fuel cell which improves the cooling process.

It should be noted that as the ribs of channels becomes smaller (e.g. the geometry D relative to geometry C), the manufacturing procedure of flow distributor on the graphite plate becomes more difficult. It can also increase the chance of a crash in the gas diffusion layer, due to the contact pressure in the assembling process. for a large size of the ribs, the gas diffusion layer may bend toward the flow channels and disturb or even stop the flow of gases inside the channels. Therefore, it is necessary to consider manufacturing restrictions on the ribs of the flow channels along with fluid flow and heat transfer rate inside the fuel cells.

The polarization curve for the PEM fuel cells associated with the geometries C and D are presented in Fig. 11. As a result, one can conclude that the performance of the fuel cell can be improved by decreasing the width of the ribs. This results in an increase in the current density and a decrease in the temperature variation and also maximum temperature value in the fuel cell. In the geometry C, as the size of ribs is large with respect to the channels, the reactants at the channel inlet and also in a part of ribs is consumed. As a result, less amount of reactant reaches to the end of channels. This leads to a non-uniform chemical reaction inside the fuel cell and decreases its performance. Therefore, the geometry D is generally better than the geometry C.

D) Comparison of Geometries with Different Depth of the Flow Channels (Geometries E and F) and Step-like Flow Channel (Geometry G)

In this section, the effects of the flow channel depth on the

current density and temperature distributions and also the performance of the fuel cell are investigated. The depths of the fluid flow channels in the geometries E and F are 0.2 and 0.3 (mm), respectively. In addition, the base depth of the flow channel in the geometry Gis 0.3 (mm) and depth of each step is 0.1 (mm). The current density distributions in different geometries of the fuel cell are shown in Figs. 12a to 12c. The variation of the current density along the anode catalyst layer is plotted in Fig. 12d. These figures indicate that the amount of available oxygen in the cathode catalyst layer is reduced by increasing the depth of the flow channels. This results in a decrease in the current density value at the cathode catalyst layer. The structure of the step-like channels helps to reduce the amount of oxygen at catalyst layer, and consequently, the current density. This is one of disadvantages of increasing the depth of flow channels which leads to a decrease in the power density and the specific power and also it makes the fuel cell more expensive. Note that as the depth of flow channels decreases, the fluid flow experiences more pressure drop during the channels.

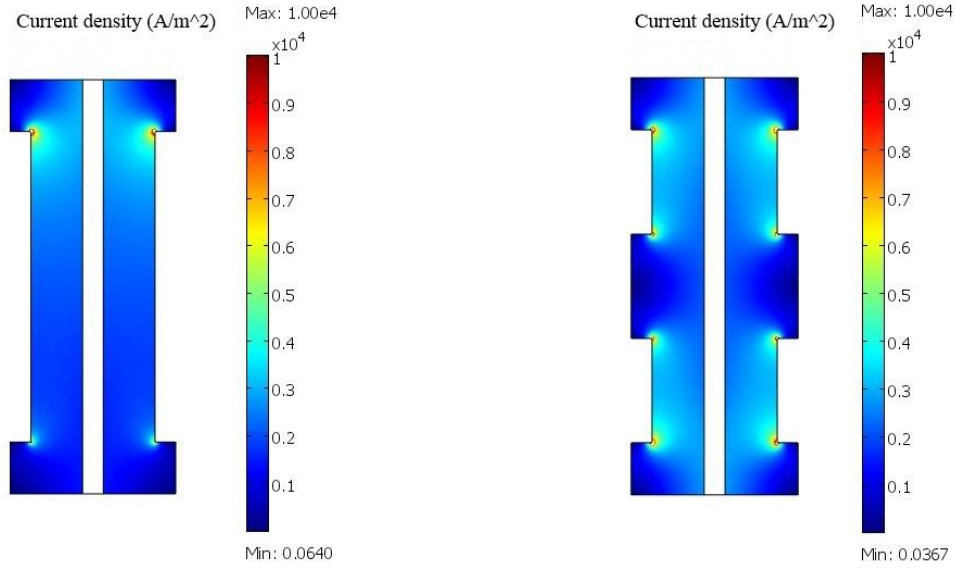

a) Geometry C **b) Geometry D**

Fig. 9. Current density distributions at the cross section of the fuel cell in geometries with different size of ribs of flow channels.

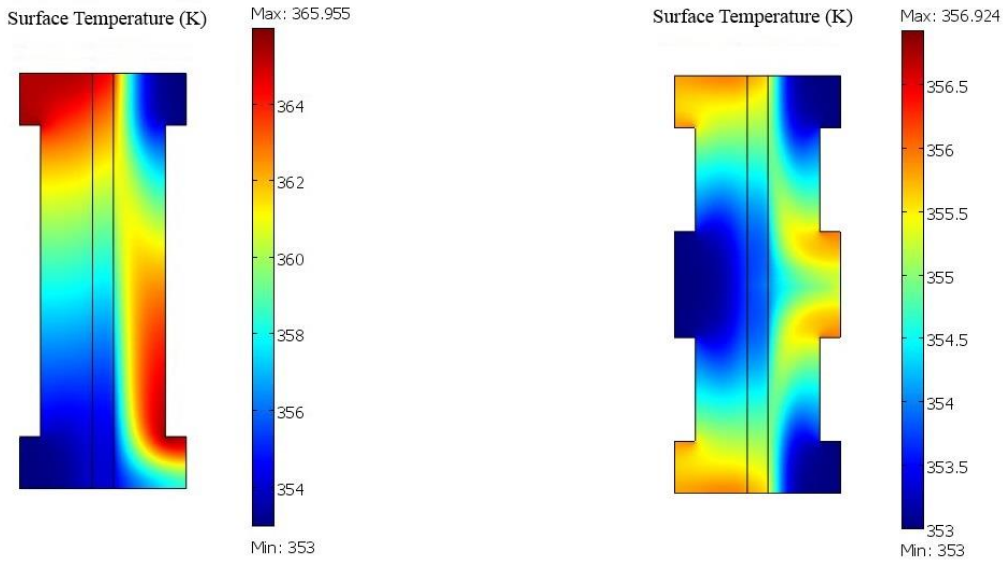

a) Geometry C **b) Geometry D**

Fig 10. Temperature distribution at the cross section of fuel cells in the geometries with different size of ribs of flow channels.

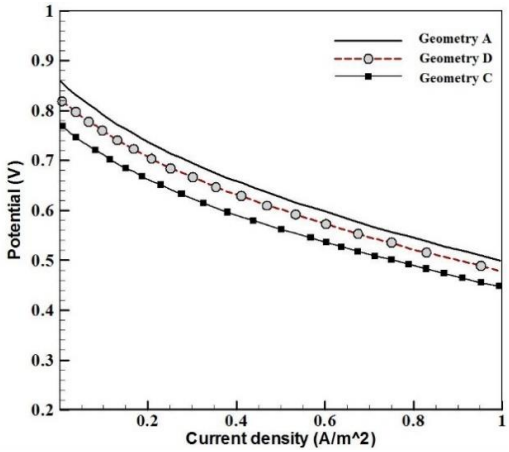

Fig. 11. Comparison of the polarization curves for the fuel cells associated with the geometries C and D.

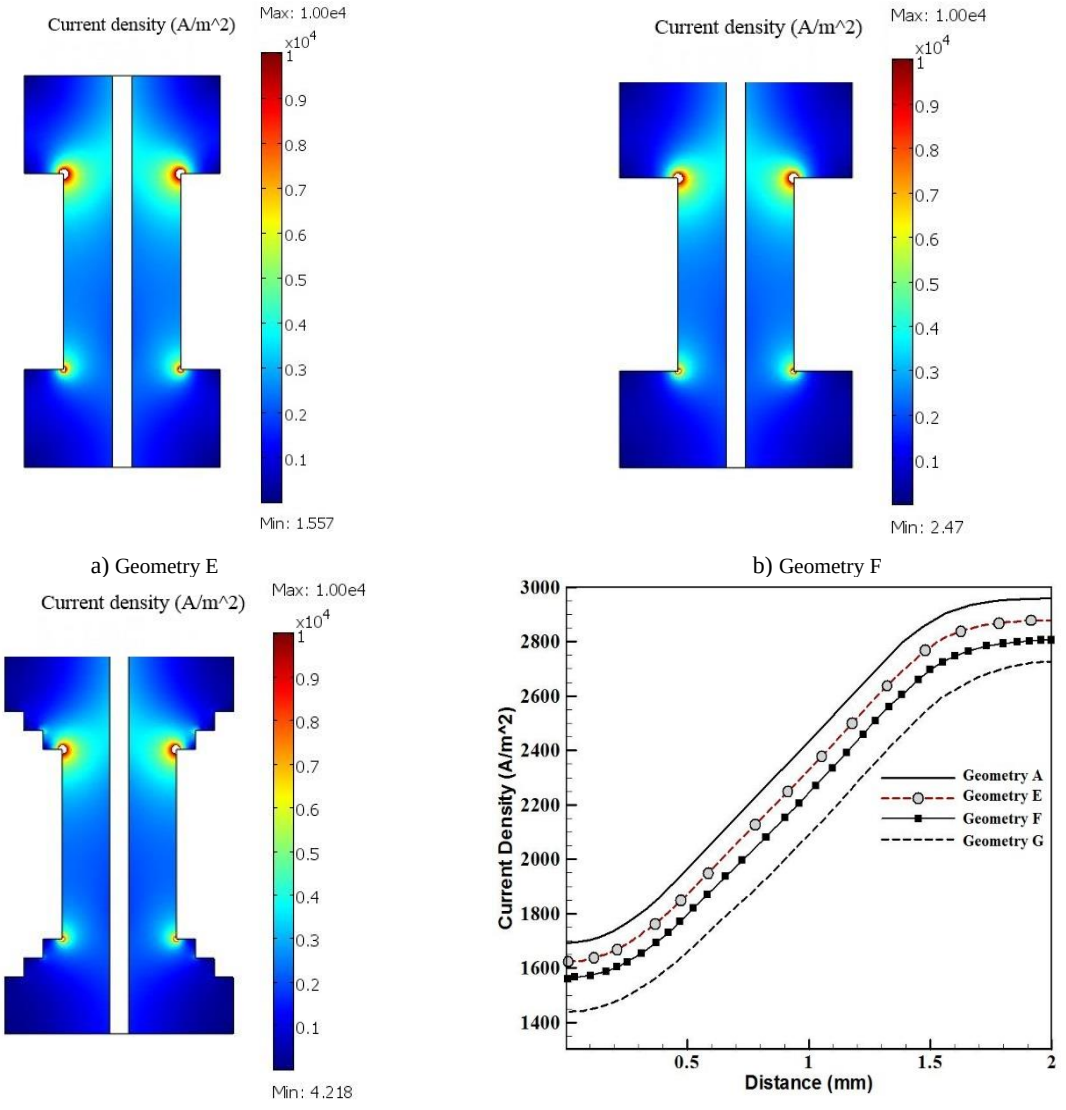

Fig. 12. Current density in different geometries of the fuel cell.

Temperature contours for geometries with different depths of the fluid flow channels and also for the step-like flow channels are represented in Figs. 13. Although the values of the maximum temperature in these geometries are nearly the same, the fuel cell with the step-like flow channels has the maximum value. In addition, the maximum temperature in geometry F is about 1 (K) more than that of geometry E. According to the current density and temperature distributions, one can conclude that increasing the depth of the flow channels is not appropriate for the PEM fuel cells. In fact, the fuel cell performance is decreased by increasing the depth of the flow channels. On the other hand, increasing the depth of the flow channels can reduce the pressure drop along the channels which is favorable. Figure 14 shows the polarization curve for the geometries E, F, and G. It can be seen that the geometry G with the step-like channels has the lowest and the geometry E has the highest electrical potential in all current density values.

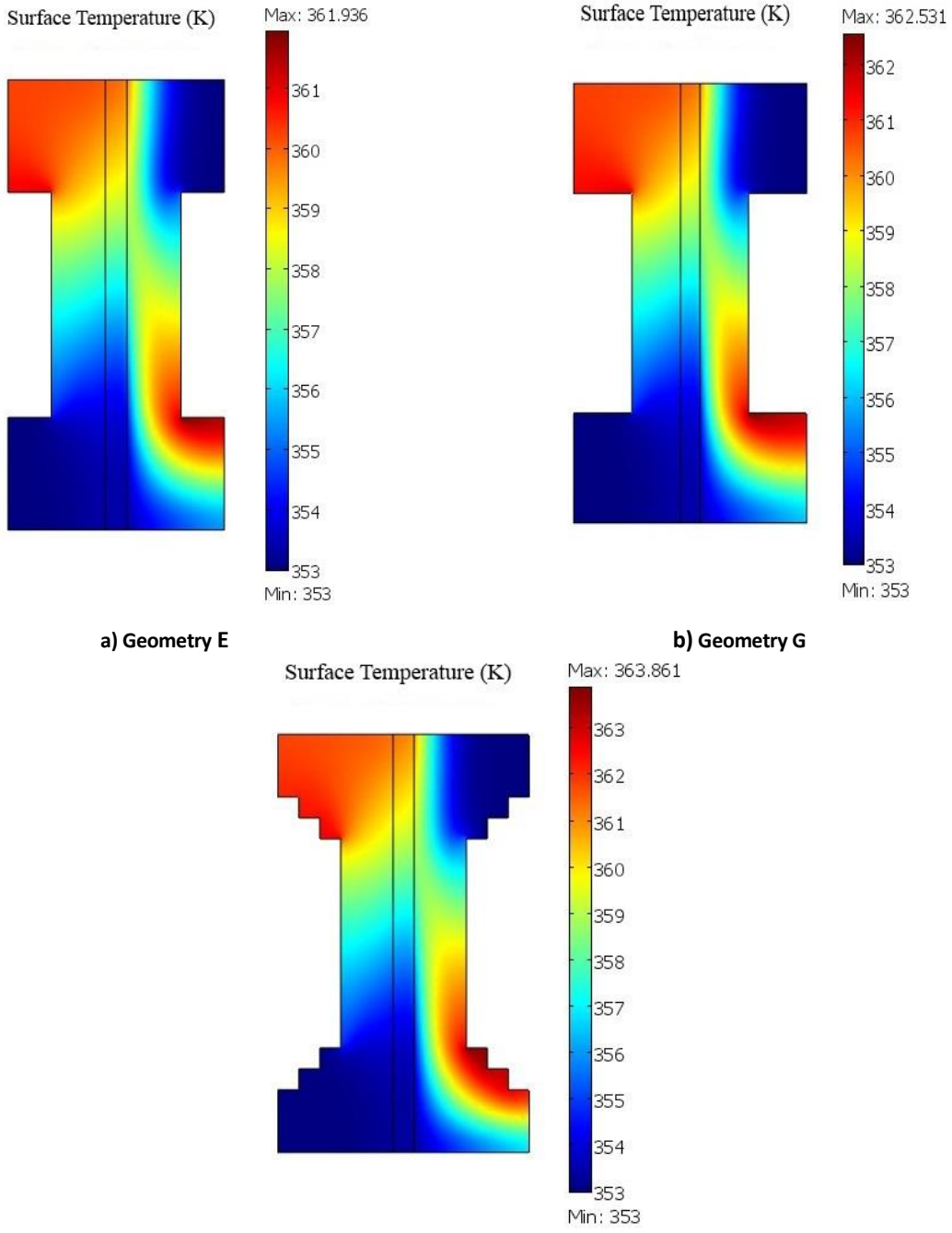

Fig. 13. Temperature in different geometries of the fuel cell.

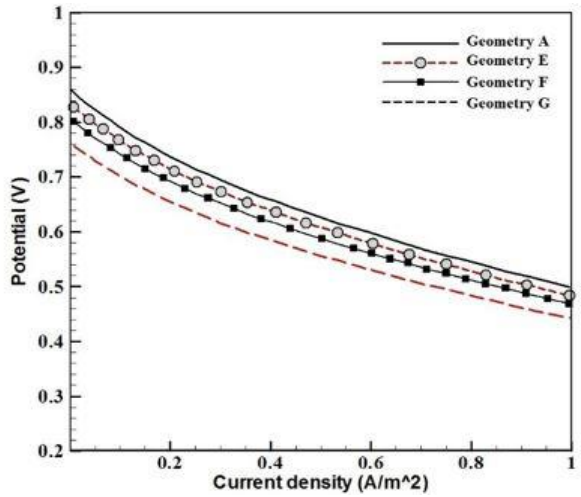

Fig. 14. Polarization curve for the geometries A, E, F, and G.

Conclusion

In the present study, the performance of the polymer electrolyte membrane fuel cell was numerically investigated. To do this, the current density and temperature distribution inside the fuel cell with different geometrical properties, including the size of the width, depth, and the ribs of the fluid flow channels, were presented and compared. In this study, geometry E was considered as initial geometry due to ease in the process of making graphite plates of fuel cell. Summary of the results of the changes in the value of the maximum current density and the maximum temperature for a fuel cell with different channel geometry and a functional voltage of 0.7V in Table3 is presented. It was shown that by decreasing the width of the ribs and the depth of flow channels and increasing the width of the flow channels (geometries A, D and B, respectively), the general performance of the PEM fuel cell (relative to the geometry E) is improved and also the maximum temperature of the cell is reduced. As shown in this table, when geometry B is used, the performance of the PEM fuel cell is better than that of the other seven cases investigated.

Table 3. Comparison all channel geometry with initial geometry (E)

Geometry	Current Density (A/m^2)	Current Density Difference with E (%)	Max Temperature (K)	Temperature Difference with E (K)
E	0.21	-	361.93	-
A	0.28	+33.3	361.1	-0.83
B	0.37	+76.2	356.46	-5.47
C	0.13	-38	365.95	+4.02
D	0.22	+4.7	356.92	-5
F	0.18	-14.3	362.53	+0.6
G	0.1	-52.4	363.86	+1.93

Conflict of Interest

There is no conflict of interest by the authors.

References

[1] R. O. Hayre, S.W. Cha, W. F. Collela, B. Prinz, *Fuel cell fundamentals*, 3rd Edition, John Wiley & Sons, New York, USA, 2016.

[2] Y. Wang, K. Chen, J. Mishler, S. Chan Cho, X.A. Cordobes Adroher, review of polymer electrolyte membrane fuel cells: Technology, applications, and needs on fundamental research. *J. Applied Energy*, vol. 88, no. 4, pp. 981-1007, 2011.

[3] M.F. Mathias, J. Roth, Diffusion media materials and characterization. *Handbook of fuel cell technology fundamentals, technology and applications*, John Wiley & Sons, New York, 2010.

[4] D. M. Bernardi and M. W. Verbrugge, Mathematical model of a gas diffusion electrode bonded to a polymer electrolyte, *AIChe Journal*, vol. 37, pp. 1151-1163, 1991.

[5] R. Boddu, U. K. Marupakula, B. Summers, P. Majumdar, Development of bipolar plates with different flow channel configurations for fuel cells, *Journal of Power Sources*. vol. 182, no. 2, 1083-1092, 2009.

[6] X. D. Wanga, X. X. Zhanga, W. M. Yanb, D. J. Leec, A. Sud, Determination of the optimal active area for proton exchange membrane fuel cells with parallel, interdigitated or serpentine designs, *international journal of hydrogen energy*, vol. 34, no. 9, pp. 3823-3829, 2009.

[7] S. M. Baek, D. H. Jeon, J. H. Nam and C. J. Kim, Pressure drop and flow distribution characteristics of single and parallel serpentine flow fields for polymer electrolyte membrane fuel cells, *Journal of Mechanical Science and Technology*. 26 (9) (2012),2995-3006.

[8] S. Um, C. Y. Wang, and K. S. Chen, "Computational fluid dynamics modeling of proton exchange membrane fuel cell," *Journal of the Electrochemical society, vol.* 147 no. 12, pp. 4485-4493, 2000.

[9] J. P. Owejan, T. A. Trabold, D. L. Jacobson, M. Arif, S. G. Kandlikar, "Effects of flow field and diffusion layer properties on water accumulation in a PEM fuel cell," *International Journal of Hydrogen Energy*, vol. 32, pp. 4489 – 4502, 2007.

[10] Z. M. Wan, J. H. Wan, J. Liu, "Water recovery and air humidification by condensing the moisture in the outlet gas of a proton exchange membrane fuel cell stack," *Applied Thermal Engineering*, Vol. 42, pp. 173-178, 2012.

[11] S. Rowshanzamir, M. H. Eikani, M. Khoshnoodi and T. Eshagh Nimvar, "A Parametric Study of the PEM Fuel Cell Cathode," *International journal of Engineering Science (IUST)*, vol. 19, no. 5-2, pp. 73-81, 2008.

[12] L.K. Kwac and H.G. Kim, "Investigation of gas flow characteristics in proton exchange membrane fuel cell," *Journal of Mechanical Science and Technology*, vol. 22, pp.156

1-1567, 2008.

[13] M. Ameri, P. Oroojie, "Two Dimensional PEM Fuel cell Modeling at different Operation Voltages," *World Renewable Energy Congress*, Sweden, 2011.

[14] X. Zhang, A. Higier, Xu. Zhang and H. Liu, "Experimental Studies of Effect of Land Width in PEM Fuel Cells with Serpentine Flow Field and Carbon Cloth," *Energies*, pp. 471-481, 2019.

[15] N. Ahmadi, S. Rezazadeh, A. Dalvand and I. Mirzaee, "Study of effect of gas channels geometry on the performance of poly polymer electrolyte membrane fuel cell," *Periodical Polytechnic Chemical Engineering*, vol. 62, no. 1, pp. 97-105, 2018.

[16] M. Muthukumar, P. Karthikeyau, M. Vairavel, C. Loganathan, S. Praveen kumar and A.P. Sentil kumar, "Numerical Studies on PEM Fuel Cell with Different Landing to Channel Width of Flow Channel," *Science Direct, Procedia Engineering*, vol. 97, pp. 1534-1542, 2014.

[17] H. Liu, P. Lia, K. Wang, "Optimization of pem fuel cell flow channel dimensions, Mathematic modeling analysis and experimental verification," *International Journal of Hydrogen, Energy*, vol. 38, pp. 9835-9846, 2013.

[18] V. Lakshminarayanan and P. Karthikeygan, "Optimization of Flow Channel Design and Operation Parameters on Proton Exchange Membrane Fuel Cell Using Matlab," *Periodical Polytechnic Chemical Engineering*, vol. 60, no. 3, pp. 173-180, 2016.

[19] R. Hadjadj and W. Kaabar, "Numerical Investigation of Flow Field in Proton Exchange Membrane Fuel Cell at Different Channel Geometries," *Journal of Engineering Science and Technology*, vol.13, no. 4, pp. 1070-1089, 2018

[20] COMSOL AB, *Comsol Metaphysics Manual*, Ver.3.3: The proton exchange membrane fuel cell, Burlington, MA, USA, 2006.

[21] P. Mondal and Md. A. AL Ahad, "Analysis of Electro-Thermal Characteristics of a Conductive Layer with Cracks and Holes, Global," *Journal of Researches in Engineering Mechanical and Mechanics Engineering*, vol. 14, no.1, 2014 .